An epi-evolutionary model to predict spore-producing pathogens adaptation to quantitative resistance in heterogeneous environments

Ramsès Djidjou-Demasse[a],Jean-Baptiste Burie[d,e], Arnaud Ducrot[c], Sébastien Lion[b], Quentin Richard[a], Frédéric Fabre[f]

[a] *Univ. Montpellier, MIVEGEC, IRD, CNRS, Montpellier F-34394, France*

[b] *CEFE, CNRS, Univ. Montpellier, Univ. Montpellier 3 Paul-Valéry, EPHE, IRD, Montpellier F-34293, France*

[c] *Univ. Normandie, UNIHAVRE, LMAH, FR-CNRS-3335, ISCN, 76600 Le Havre, France*

[d] *Univ. Bordeaux, IMB, UMR 5251, Talence F-33400, France*

[e] *CNRS, IMB, UMR 5251, Talence F-33400, France.*

[f] *INRAE, Bordeaux Sciences Agro, UMR SAVE, Villenave d'Ornon F-33882, France*

September 16, 2020

Abstract

In contrast to the many theoretical studies on the adaptation of plant pathogens to qualitative resistances, few studies have investigated how quantitative resistance selects for increased pathogen aggressiveness. We formulate an integro-differential model with nonlocal effects of mutations to describe the evolutionary epidemiology dynamics of spore-producing pathogens in heterogeneous agricultural environments sharing a well-mixed pool of spores. Parasites reproduce clonally and each strain is characterized by pathogenicity traits corresponding to the epidemic process: (i) infection efficiency and (ii) sporulation curve (including the latent period, the total spore production and the shape of the sporulation curve). We first derive a general expression of the basic reproduction number $\mathcal{R}_0$ for fungal pathogens in heterogeneous host environments. Next, by characterizing evolutionary attractors, we investigate how the choice of quantitative resistances altering pathogenicity traits impacts the evolutionary dynamics of the pathogen population both at equilibrium and during transient epidemiological dynamics. We show that evolutionary attractors of the model coincide with local maxima of the $\mathcal{R}_0$ only for traits involved in the sporulation curve. Quantitative resistance impacting the sporulation curve will always select a monomorphic population while dimorphism can occur with resistance altering infection efficiency. We also highlight how the shape of the relationship between the latent period and the total number of spores produced during the infectious period, impacts resistance durability and how to take advantage of evolutionary dynamics to increase the durability of quantitative resistance. Our analyses can guide experimentations by providing testable hypotheses and help plant breeders to design breeding programs.

Key words. Basic reproduction number; Resistance durability; Adaptive dynamics; Spores-producing pathogens; Quantitative resistance.

1 Introduction

Resistance to parasites, i.e. the capacity of a host to decrease its parasite development (Raberg et *al.*, 2009), is a widespread defense mechanism in plants. Qualitative resistance usually confers disease immunity in such a way that parasites exhibit a discrete distribution of their disease phenotype ("cause disease" versus "do not cause disease") (McDonald & Linde, 2002). Quantitative resistance leads to a reduction in disease severity (Poland et *al.*, 2009; St. Clair, 2010) in such a way that parasites exhibit a continuous distribution of their quantitative pathogenicity (McDonald & Linde, 2002; St. Clair, 2010; Lannou, 2012). Quantitative pathogenicity, also termed aggressiveness, can be estimated in laboratory experiments through the measure of a small number of pathogenicity traits (Lannou, 2012) expressed during the basic steps of the host-pathogen interaction. Quantitative resistance has gained interest in plant breeding for pathogen control in low-input cropping systems, in particular due to their supposed higher durability compared to qualitative resistance (Niks et *al.*, 2015). However plant pathogens also adapt to quantitative resistance (see Pilet-Nayel et *al.* (2017) for a review). The resulting gradual "erosion"

of resistance efficiency (McDonald & Linde, 2002) corresponds, from the pathogen side, to a gradual increase in quantitative pathogenicity.

Few theoretical studies have investigated how the deployment of quantitative resistance in agrosystems impacts pathogen aggressiveness (Iacono et *al.*, 2012; Bourget *al.*, 2015; Rimbaud et *al.*, 2018). These studies must address the fundamental short- and long-term objectives of sustainable management of plant diseases (Zhan et *al.*, 2015; Rimbaud et *al.*, 2018): the short-term goal focuses on the reduction of disease incidence, whereas the longer-term objective is to reduce the rate of evolution of new pathotypes. The evolutionary epidemiology analysis are well-suited for this purpose (Day & Proulx, 2004). Essentially inspired by quantitative genetics, it accounts for the interplay between epidemiological and evolutionary dynamics on the same time scale. As such it can be used to monitor the simultaneous dynamics of epidemics and evolution of any set of pathogen life-history trait of interest. It can also handle heterogeneous host populations resulting, for example, from differences in their genetic composition (Gandon & Day, 2007). This is typically the case of field mixtures, where several cultivars are cultivated in the same field, and of landscapes mosaics, with cultivars cultivated in different fields.

In this article, we follow this approach and study the evolutionary epidemiology of spore-producing pathogens in heterogeneous agricultural environments. Plant fungal pathogens (*sensu lato, i.e.* including Oomycetes) are typical spore-producing pathogens responsible for nearly one third of emerging plant diseases (Anderson et *al.*, 2004). Here we use an integro-differential model where the pathogen traits are represented as a function of a N-dimensional phenotype. This model extends previous results of Djidjou-Demasse et *al.* (2017) to heterogeneous plant populations mixing cultivars with different quantitative resistances. First, we investigate how the deployment of quantitative resistances altering different pathogenicity traits impact the pathogen population structure at equilibrium. This question is addressed by characterizing the evolutionary attractors of the coupled epidemiological evolutionary dynamics. A particular emphasis will be put here on the differences between the cornerstone concepts of $\mathcal{R}_0$ in epidemiology (Diekmann et *al.*, 1990; van den Driessche & Watmough, 2008) and invasion fitness in evolution (Dieckmann, 2002; Diekmann et *al.*, 2005; Geritz et *al.*, 1998; Metz et *al.*, 1996; Nowak & Sigmund, 2004). Secondly we investigate how the deployment of quantitative resistances impacts the transient behavior of the coupled epidemiological evolutionary dynamics.

Category	Description	Unit
Notations		
$N_c \geq 2$	Total number of host classes	
$k \in 1, 2, \cdots, N_c$	Index on host class	
N	Dimension of the phenotype space	
$x \in \mathbb{R}^N$	Label on the pathogen strain.	
a	Time since infection	
States variables		
$S_k(t)$	Density of healthy tissue of host k at time t.	
$i_k(t, a, x)$	Density of infected tissue of host k at time t infected since time a by strain x	
$A(t, x)$	Density of airborne pool of pathogen spores of strain x at time t.	
Parameters		
Λ	Birth rate of healthy host tissue	$\text{HTD} \cdot \text{Tu}^{-1}$
θ	Death rate of host tissue	Tu^{-1}
δ	Rate at which spore becomes unviable	Tu^{-1}
$d_k(a, x)$	Disease induced mortality of host k infected since a by strain x	Tu^{-1}
$\beta_k(x)$	Infection efficiency of pathogen strain x on host k	$\text{SD}^{-1} \cdot \text{Tu}^{-1}$
$p_k(x)$	Total number of spores produced by pathogen strain x on host k	$\text{SD} \cdot \text{HTD}^{-1}$
$\tau_k(x)$	Latent period of pathogen strain x on host k	Tu
$\lambda_k(x)$	Sporulation curve shape of strain x on host k : rate of sporulation events	Tu^{-1}
$n_k(x)$	Sporulation curve shape of strain x on host k : number of sporulation events	unitless
φ_k	Proportion of host k at the disease-free equilibrium	unitless
ε	Distance beyond which non-local mutations become "negligible"	unitless
$m_\varepsilon(x - y)$	Mutation probability from pathogen strain x to y	unitless

Tu= time unit; SD= spores density; HTD=host tissue density

Table 1: Main notations, state variables and parameters of the model.

2 An epi-evolutionary model structured by age of infection and strain

2.1 Host and pathogen populations

We consider an heterogeneous host population with $N_c \geq 2$ host classes infected by a polymorphic spore-producing pathogen population. Here, host heterogeneity may refer to different host classes, typically plant cultivars, but more generally it can handle different host developmental stages, sexes, or habitats. The host population is further subdivided into two compartments: susceptible or healthy host tissue (S) and infectious tissue (I). In keeping with the biology of fungal pathogens, we do not track individual plants, but rather leaf area densities (leaf surface area per m^2). The leaf surface is viewed as a set of individual patches corresponding to a restricted host surface area that can be colonized by a single pathogen individual. Thus only indirect competition between pathogen strains for a shared resource is considered. Spores produced by all infectious tissues are assumed to mix uniformly in the air. They constitute a well-mixed pool of spores landing on any host class according to the law of mass action. Thus the probability of contact between a spore and host k is proportional to the total susceptible leaf surface area of this host. The density of airborne pool of spores is denoted by A.

The parasite is assumed to reproduce clonally. Its population is made of a set of genetic variant termed thereafter strains. Each strain with phenotype x is characterised, on each host class, by pathogenicity traits that describe the basic steps of the disease infection cycle : (i) infection efficiency $\beta_k(x)$, *i.e.* probability that a spore deposited on a receptive host surface produces a lesion and (ii) sporulation curve $r_k(a,x)$. In line with the biology of plant fungi (van den Bosch et *al.*, 1988; Sache et *al.*, 1997; Kolnaar & Bosch, 2011; Segarra et *al.*, 2001), a gamma sporulation curve defined by four parameters is assumed : (i) latent period $\tau_k(x)$, (ii) total number of spores produced $p_k(x)$ during the infectious period, (iii) number of repeated sporulation events occurring on an individual foliar lesion $n_k(x)$ and (iv) rate of sporulation events $\lambda_k(x)$. Parameters n_k and λ_k define the time shape of the sporulation curve by distributing the total amount of spores produced by a lesion (p_k) over its average infectious period (n_k/λ_k) (Figure 1A). Previous hypothesis lead to the following sporulation function :

$$r_k(a,x) = \begin{cases} p_k(x)\frac{\lambda_k^{n_k(x)}(a-\tau_k(x))^{n_k(x)-1}\exp[-\lambda_k(x)(a-\tau_k(x))]}{\Gamma[n_k(x)]} & \text{if } a > \tau_k(x), \\ 0 & \text{otherwise.} \end{cases} \tag{2.1}$$

2.2 The model

We introduce a set of integro-differential equations modeling the epidemiological and the evolutionary dynamics of the host and pathogen populations just described. Table 1 lists the state variables and parameters of the model. The general formulation used encompasses several simpler models of the literature (Appendix C). A key feature of the model is to explicitly track both the age of infection and the pathogen strain. This leads to a non-local age-structured system of equations posed for time $t > 0$, age since infection $a > 0$ and phenotype $x \in \mathbb{R}^N$,

$$\begin{cases} \partial_t S_k(t) = \varphi_k \Lambda - \theta S_k(t) - S_k(t)\displaystyle\int_{\mathbb{R}^N} \beta_k(y)A(t,y)\mathrm{d}y, \\ (\partial_t + \partial_a)\, i_k(t,a,x) = -\left(\theta + d_k(a,x)\right) i_k(t,a,x), \\ i_k(t,0,x) = \beta_k(x)S_k(t)A(t,x), \\ \partial_t A(t,x) = -\delta A(t,x) + \displaystyle\sum_{k=1}^{N_c}\int_{\mathbb{R}^N}\int_0^\infty m_\varepsilon(x-y)r_k(a,y)i_k(t,a,y)\mathrm{d}a\mathrm{d}y. \end{cases} \tag{2.2}$$

$S_k(t)$ is the density of healthy tissue in host k at time t, $i_k(t,a,x)$ the density of tissue in host k that was infected at time $t-a$ by a pathogen with phenotype x, and $A(t,x)$ denotes the density of spores with phenotype x at time t. Susceptible hosts are produced at rate $\Lambda > 0$ and φ_k is the proportion of the host k at the disease-free equilibrium in the environment. With disease, susceptible hosts can become infected by airborne spores. The total force of infection on a host k is $h_k(t) = \int \beta_k(y)A(t,y)\mathrm{d}y$. Airborne spores produced by infected hosts become unviable at rate $\delta > 0$. Healthy hosts die at rate $\theta > 0$ (regardless of their class) and infected hosts at rate $\theta + d_k(a,x)$, where $d_k(a,x)$ is the disease-induced mortality. Hosts infected by strain y produce airborne spores with phenotype x at a rate $m_\varepsilon(x-y)r_k(a,y)$, where $r_k(a,y)$ is the sporulation function, which depends on host class, age of infection and parasite phenotype and $m_\varepsilon(x-y)$ is the probability of mutation from phenotype y to phenotype x. Thus mutations randomly displace strains into the phenotype space at each infection cycle (*i.e.* generation) according to the kernel m_ε. m_ε depends on a small parameter $\varepsilon > 0$ representing the mutation variance in the phenotypic space. To fix ideas, a multivariate Gaussian distribution $m = N(0,\Sigma)$ leads to $m_\varepsilon(x-y) = \frac{1}{\varepsilon^N} m\left(\frac{x-y}{\varepsilon}\right)$. The covariance terms

Σ can allow us to take into account correlations between pathogen life-history traits (Gandon , 2004). Note that the kernel is not restricted to Gaussian distributions, provided it satisfies some properties such as positivity and symmetry (Appendix B).

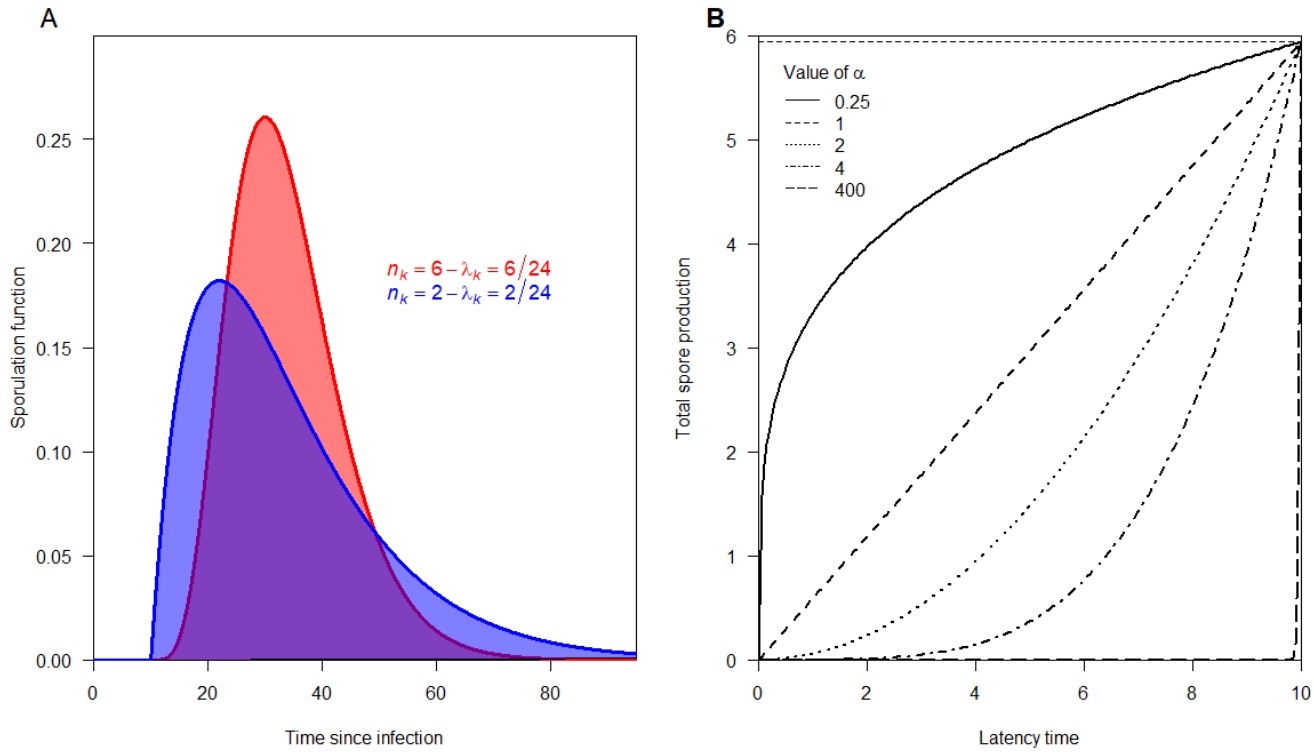

Figure 1: **A** Shapes of gamma sporulation function $r_k(a, x)$ with latent period $\tau_k = 10$ and total spore production during the whole infectious period $p_k = 5.94$ as a function of n_k and λ_k. The average infectious period (n_k/λ_k) is 24 for both functions. **B** Shape of the relationship between latency duration τ_k and total spore production p_k as a function of α. The maximal spore production $p_{max} = 5.94$ is assumed to be obtained for the latency duration $\tau_{max} = 10$.

3 Fitness function and evolutionary attractors

3.1 The fitness function

The basic reproduction number, usually denoted $\mathcal{R}_0$, is defined as the total number of infections arising from one newly infected individual introduced into a healthy (disease-free) host population (Diekmann et *al.*, 1990; Anderson, 1991). The disease-free equilibrium density of susceptible hosts in class k is $S_k^0 = \varphi_k \Lambda/\theta$. In an environment with N_c host classes, a pathogen with phenotype x will spread if $\mathcal{R}_0(x) > 1$, with

$$\mathcal{R}_0(x) = \sum_{k=1}^{N_c} \mathcal{R}_0^k(x), \tag{3.3}$$

where the quantity $\mathcal{R}_0^k(x) = \Psi_k(x) S_k^0$ is the basic reproduction number of a pathogen with phenotype x in the host k, and the fitness function Ψ_k is given by

$$\Psi_k(x) = \frac{1}{\delta}\beta_k(x) \int_0^\infty r_k(a, x) \exp\left(-\theta a - \int_0^a d_k(\sigma, x) \mathrm{d}\sigma\right) \mathrm{d}a, \tag{3.4}$$

for all $k \in \{1, \ldots, N_c\}$. The quantity $\Psi_k(x)$ is the absolute fitness, or reproductive value, of a pathogen with phenotype x landing on host k (Appendix D). Note that $\exp\left(-\theta a - \int_0^a d_k(\sigma, x)\mathrm{d}\sigma\right)$ is the probability that a lesion is alive at age a. Once multiplied by $r_k(a, x)$ and integrated over all infection age a it gives the total number of

spores truly produced by a lesion during its life time while $p_k(x)$ is the number of spores potentially produced if the lesion stay alive during the whole infectious period.

Assuming that d_k does not depend on the age of infection and a gamma sporulation function, we obtain the simpler expression

$$\Psi_k(x) = \frac{1}{\delta} \times \beta_k(x) \times e^{-(\theta+d_k(x))\tau_k(x)} \times p_k(x) \times \left(\frac{\lambda_k}{\lambda_k+\theta+d_k(x)}\right)^{n_k}. \tag{3.5}$$

This equation traduces that (i) during its life time $1/\delta$, (ii) a propagule infects a leaf area at rate β_k, (iii) this infected area survives the latent period with probability $e^{-(\theta+d_k)\tau_k}$, (iv) achieves n_k sporulation events with probability $\left(\frac{\lambda_k}{\lambda_k+\theta+d_k}\right)^{n_k}$ and (v) produces a total number of spores p_k during the infection period. If furthermore r_k is a constant (*i.e.* $r_k(a,x) = p_k(x)$ and $d_k(a,x) = d_k(x)$ for all a), we recover the classical expression of $\mathcal{R}_0$ for SIR models (Day, 2002) with

$$\Psi_k(x) = \frac{\beta_k(x)p_k(x)}{\delta(\theta+d_k(x))}$$

3.2 Evolutionary attractors

$\mathcal{R}_0$ can be used to study the spread of a pathogen strain x in an *uninfected* host population. To study the spread of a new mutant strain in a host population *already infected* by a resident strain x, and to characterize pathogen's evolutionary attractors among a large number of pathogen strains, we can use the adaptive dynamics methodology and calculate invasion fitness (Dieckmann, 2002; Diekmann et *al.*, 2005; Geritz et *al.*, 1998; Metz et *al.*, 1996; Nowak & Sigmund, 2004).

Here, we work in generation time and use the lifetime reproductive success of a rare mutant as a fitness proxy. Once the pathogen with phenotype x spreads, let us assume that the population reaches a monomorphic endemic equilibrium denoted by $E^x = (S_k^x, i_k^x(\cdot), A^x)_{k=1,\cdots N_c}$. The calculations of E^x, the environmental feedback of the resident x, are detailed in Appendix D. A rare mutant with phenotype y will invade the resident population infected by the strain x if the invasion fitness $f_x(y)$ of y in the environment generated by x is such that

$$f_x(y) = \mathcal{R}(y, E^x) - 1 > 0,$$

where

$$\mathcal{R}(y, E^x) = \sum_{k=1}^{N_c} S_k^x \Psi_k(y). \tag{3.6}$$

Quantities $\mathcal{R}(y, E^x)$ and $\mathcal{R}_0(y)$, given by equations (3.3) and (3.6), have a strong analogy. Both expressions are basic reproduction numbers that measure the weighted contribution of the pathogen to the subsequent generations, but while $\mathcal{R}_0(y)$ is calculated in the disease-free environment, $\mathcal{R}(y, E^x)$ is calculated in the environment E^x. Noteworthy $\mathcal{R}(y, E^x)$ takes the form of a sum of the mutant pathogen's reproductive success in each host class as between-class transmission can be written as the product of host susceptibility times pathogen transmissibility. This is equivalent to the more general statement that pathogen propagules all pass through a common pool, as in our model in the compartment A (Rueffler & Metz (2013)). However, this property is not generally true as shown by Gandon (2004) in a two-class model.

In general, finding the evolutionary attractors of host-pathogen systems is mostly based on properties of the invasion fitness on an adaptive landscape (Diekmann et *al.*, 2005; Geritz et *al.*, 1997, 1998; Nowak & Sigmund, 2004). A Pairwise Invasibility Plot (PIP) must then be used to characterize evolutionary attractors. However, when infection efficiencies do not differ between host classes (*i.e.* $\beta_k = \beta$, for all k), model (2.2) admits an optimisation principle (Mylius & Diekmann, 1995; Metz et *al.*, 2008; Lion & Metz, 2018; Gyllenberg & Service, 2011). More precisely, the evolutionary attractors of the model coincide with the maxima of the $\mathcal{R}_0$ (Appendix F).

4 Application to the durability of quantitative resistances impacting sporulation or infection efficiency

4.1 Case study : deployment of a quantitative resistance

We consider two habitats corresponding to a susceptible (S) and a resistant (R) cultivars. The S cultivar has been cultivated alone during a long time. As a result, it is infected by a monomorphic pathogen population A_0. At

$t = 0$, a fraction $\varphi \in (0, 1)$ of the S cultivar is replaced by the R cultivar. Two scenarios were then considered: the quantitative resistance can either alter the total spore production (SP scenario) or the infection efficiency (IE scenario). To illustrate how these scenarios impact the coupled epidemiological and evolutionary dynamics we need to specify the fitness of a given pathogen strain x on each habitat. We used the following unnormalized Gaussian functions

$$\omega_S(x) = \omega_{\max} \times \exp\left(-\frac{(x+\mu)^2}{2\sigma_S^2}\right) \quad \text{and} \quad \omega_R(x) = \omega_{\max}(1-c) \times \exp\left(-\frac{(x-\mu)^2}{2\sigma_R^2}\right),$$

where $-\mu$ and μ are optimal phenotypes on S and R cultivars, $\omega_{\max}$ is the optimal value of the pathogenicity trait on the S cultivar, and $c \in [0, 1]$ quantified the cost of the pathogen adaptation on the R cultivar. The maximum points of $\mathcal{R}_0^S$ and $\mathcal{R}_0^R$ are given by $\mu_S = -\mu$ and $\mu_R = \mu$ and accordingly, we have $\omega_S(\mu_S) = \omega_{\max}$ and $\omega_R(\mu_R) = \omega_{\max}(1-c)$. Furthermore, $1/\sigma_S^2$ and $1/\sigma_R^2$ define the selectivity of the S and R habitats. On the R cultivar it defines the spectrum of action of the quantitative resistance on different pathogen strains (Pilet-Nayel et *al.*, 2017). Altogether, the parameters μ, c, σ_S^2 and σ_R^2 define the efficiency of the quantitative resistance.

A positive correlation has been sometimes observed for plant fungi between the duration of the latent period and fecundity (Pariaud et *al.*, 2013). This relationship describes a phenotypic trade-off because short latent period and high sporulation probability represent fitness advantages. We introduced this relationship in the SP scenario assuming that the maximal spore production on each cultivar is obtained for the latency duration τ_{max}. The aggressiveness components $p_k(x)$ and $\tau_k(x)$ (with $k \in \{S, R\}$) of a pathogen strain x are then linked as follow

$$p_S(x) = p_{max}\left(\frac{\tau_S(x)}{\tau_{max}}\right)^{\alpha} \quad \text{and} \quad p_R(x) = p_{max}(1-c)\left(\frac{\tau_R(x)}{\tau_{max}}\right)^{\alpha},$$

where α define the shape of the trade-off (Figure 1B). For example $\alpha = 2$ is suggested by Pariaud et *al.* (2013).

Simulations were initiated with a Gaussian density A_0 centered around the optimal phenotype on the S cultivar. We illustrated how contrasted values of μ (a proxy of resistance efficiency), φ (defining the deployment strategy) and α (shape of the trade-off between sporulation and latency) affect the evolutionary dynamics of the pathogen. We estimated two times to characterize these dynamics. We estimated the time T_{shift} of emergence of the adapted strains as as the time t from which $A(t, \mu_R)/\left(A(t, \mu_S) + A(t, \mu_R)\right)$ is always $\geq 5\%$. Following (Rimbaud et *al.*, 2018), we also estimated the durability of the R cultivar as the time T_{inf} when at least 5% of the leaf area density of the R cultivar is infected, *i.e.* time t from which $\int\int i_R(t, a, x)\mathrm{d}a\mathrm{d}x/\left(S_R(t) + \int\int i_R(t, a, x)\mathrm{d}a\mathrm{d}x\right)$ is always $\geq 5\%$. In practice this is the time when the erosion of the quantitative resistance become detectable in the field. All model parameters and initial conditions used for the simulations are summarized in Table 2. Parameters for pathogenicity traits do not fit a particular pathogen species but rather a typical biotrohpic foliar fungal diseases such wheat rusts on susceptible cultivars. Following Rimbaud et *al.* (2018), we define an infection efficiency of 0.2 and the duration of the latent and infectious periods to 10 and 24 days, respectively. Finally the total spore production was set in order to obtain an $\mathcal{R}_0$ of 30 in an environment with only the S cultivar (Mikaberidze et *al.*, 2016).

4.2 Effect of quantitative resistance impacting sporulation

When the quantitative resistance impacts total spore production, the $\mathcal{R}_0$ optimization principle holds (Section 3.2): the population always becomes monomorphic around an evolutionary attractor characterized by the maximum of the global $\mathcal{R}_0$ function. However the characteristics of the quantitative resistance (as determined among other by μ) and its deployment strategy (as determined by φ) impact the shape of $\mathcal{R}_0$ (number of modes and their steepness) and the underlying transient dynamics (Figure 2).

The choice of μ and φ can lead to a shape of $\mathcal{R}_0$ with an unique maximum, located at $\mu^*(\mu_S < \mu^* < \mu_R)$. The evolutionary attractor will then correspond to a generalist pathogen (Figure 2 A). The fast transient dynamics observed on simulations, with a pathogen population rapidly concentrating around μ^* (Figure 2 B,C), corresponds to a fast erosion T_{inf} of the quantitative resistance (expressed here as a number of asexual reproduction cycle). The time to erosion is quickly followed by the time to emergence T_{shift} of the adapted strain in the pathogen population (Figure 2 C).

Other choice of μ and φ can lead to a shape of $\mathcal{R}_0$ function with two local maxima. $\mathcal{R}_0$ is maximized (globally) by a single phenotype around μ_R but a local maximum also exists around μ_S (Figure 2 D). The $\mathcal{R}_0$ maximization principle indicates that μ_R is the evolutionary attractor. This phenotype is a specialist of the R cultivar. The pathogen population lives for a relatively long time around the initially dominant phenotype μ_S and then shifts by mutation on μ_R (Figure 2 E,F). These dynamics occur simultaneously on the S and R cultivars. The choice of the proportion of R cultivar strongly impact the duration of the transient dynamics. Values of φ bringing closer the

Parameters		
Name	Description	Values
$-\mu$, μ	Optimal phenotype on S and R cultivars	0.055 and 0.095
φ	Proportion of R cultivar	0.52, 0.53 and 0.055 [0.05, 0.95]
α	Shape of the trade-off sporulation-latency	2 [0.25, 1, 2, 4, 400]
σ	Selectivity ratio σ_R/σ_S	5/6
c	Fitness cost on the R cultivar	0
β_{max}	Maximal infection efficiency on the S cultivar	0.2
τ_{max}	Latency period associated to maximal sporulation	10
p_{max}	Maximal spore production on the S cultivar	5.94^a
ε	Mutation variance	0.01
$m_\varepsilon(x-y)$	Probability of mutation from x to y	$\varepsilon^{-1}\exp\left[-\lvert x-y\rvert/(2\varepsilon)\right]$
Λ	Birth rate of healthy host tissue	0.35
θ	Death rate of host tissue	0.01
δ	Rate at which spore becomes unviable	1
$n_S(x), \lambda_S(x)$	Shape of the gamma sporulation curve	$n_S = 2; \lambda_S = 2/24$
$n_R(x), \lambda_R(x)$	Shape of the gamma sporulation curve	$n_R = 2; \lambda_R = 2/24$
$d_S(a,x)$, $d_R(a,x)$	Disease induced mortality	0
$1/\sigma_S^2$	Selectivity of the S cultivar	0.06^{-2}
$1/\sigma_R^2$	Selectivity of the R cultivar	$(\sigma * \sigma_S)^{-2}$
Scenario with a quantitative resistance impacting sporulation		
$p_S(x)$	Total spore production on S cultivar	$p_{max} \times f_{\mathcal{N}}(\mu, \sigma_S, x)$
$p_R(x)$	Total spore production on R cultivar	$p_{max} \times (1-c) \times f_{\mathcal{N}}(\mu, \sigma_R, x)$
$\beta_S(x), \beta_R(x)$	Infection efficiency on S and R cultivars	β_{max}, β_{max}
$\tau_S(x)$	Latent period on S cultivar	$\tau_{max}\left(\frac{p_S(x)}{p_{max}}\right)^{1/\alpha}$
$\tau_R(x)$	Latent period on R cultivar	$\tau_{max}\left(\frac{p_R(x)}{(1-c)p_{max}}\right)^{1/\alpha}$
Scenario with a quantitative resistance impacting infection efficiency		
$\beta_S(x)$	Infection efficiency on S cultivar	$\beta_{max} \times f_{\mathcal{N}}(\mu, \sigma_S, x)$
$\beta_R(x)$	Infection efficiency on R cultivar	$\beta_{max} \times (1-c) \times f_{\mathcal{N}}(\mu, \sigma_R, x)$
$p_S(x), p_R(x)$	Total spore production on S and R cultivars	p_{max}, p_{max}
$\tau_S(x), \tau_R(x)$	Latent period on S and R cultivars	τ_{max}, τ_{max}
Initial conditions		
Variable	Description	Values
$S_S(0)$	Healthy S cultivar	$(1-\varphi)\Lambda/\theta$
$S_R(0)$	Healthy R cultivar	$\varphi\Lambda/\theta$
$i_S(0,a,x)$	Infected S cultivar	0
$i_R(0,a,x)$	Infected R cultivar	0
$A(0,x)$	Pathogen spores	$\frac{40}{\sigma_S\sqrt{2\pi}} \times f_{\mathcal{N}}(\mu, \sigma_S/5, x)$

Table 2: Initial conditions and parameters used for the simulations with two habitats (S and R cultivars). Two scenarios were considered: the R cultivar can either alter the Infection Efficiency of the pathogen (IE) or its total Spore Production (SP). $f_{\mathcal{N}}(\mu,\sigma,x) = \exp[-(x-\mu)^2/(2\sigma^2)]$ stands for the unnormalized density function of the Gaussian distribution. References values given for each parameter are the one used in all simulations although stated otherwise. Values in bracket indicate the range of variation [minimum, maximum] used for the numerical exploration. ^{a} p_{max} is such that $\mathcal{R}_0(\mu_S) = 30$ for $\varphi = 0$, leading to $p_{max} = 30 \times \theta\delta\exp(\theta\tau_{max})(1+\theta/\lambda)^n/(\beta_{max}\Lambda)$.

fitness peaks (in the sense $\mathcal{R}_0(\mu_S) \lessapprox \mathcal{R}_0(\mu_R)$) will increase the time of emergence T_{shift} of the evolutionary attractor (Figure 2 G-I). However, this longer emergence time do not corresponds to an increase durability of the R cultivar.

We further studied how the times to emergence and erosion depend on the deployment strategy φ (Figure 3) for the two values of μ used previously. Noticeably, the two times behave in opposite directions: while T_{shift} drastically decreases with φ, T_{inf} increases with φ. If both quantities converge toward close values for high proportions of R cultivar, the time to emergence T_{shift} is much longer than the time to erosion T_{inf} for most deployment strategies. This difference is particularly marked for small proportions of R cultivar for which significant infections of the R cultivar rapidly occur while the emergence of the adapted strain in the air-borne spore pool is much slower (Figure 3 A versus B). Moreover, we also studied how the shape of the trade-off between sporulation and latency α impact these times (Figure 3). Its effect, negligible for low values of φ, increases with the proportions of R cultivar deployed. In these configurations, a detailed knowledge of the shape of this trade-off is notably important for managing the durability of quantitative R characterized by weak efficiencies (in the sense of μ).

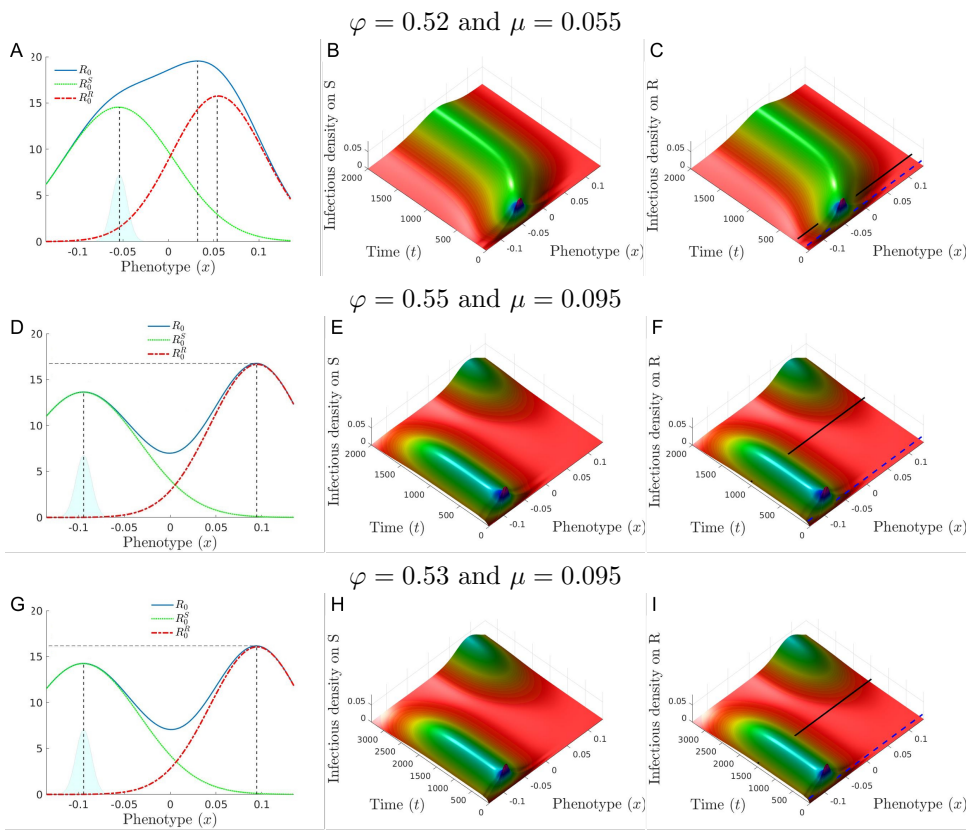

Figure 2: Evolutionary epidemiology dynamics when the resistance impacts the total spore production for three choices of μ and φ. **A-C** With $\mu = 0.055$ and $\varphi = 0.52$, the fitness function is unimodal with a maximum located between μ_S and μ_R (panel A). At $t = 0$, the pathogen population is essentially concentrated around μ_S following the light blue Gaussian distribution A_0. The dynamics of the density of infected tissue and the phenotypic composition of the pathogen population in the S and R cultivars are displayed in panels B and C, respectively. The dash-blue and black lines in panel C correspond to T_{inf} and T_{shift} respectively. **D-F** Same as **A-C** with $\mu = 0.095$ and $\varphi = 0.55$. The fitness function is bimodal with a unique global maximum at μ_R but a local maximum also exists around μ_S. **G-I** Same as **D-F** with $\mu = 0.095$ and $\varphi = 0.53$ which implies that the local maximum at μ_S is closer to μ_R compared to panels **D-F**. For all panels, $\alpha = 2$, $c = 0$, $\sigma = 5/6$ and other parameters are set to their reference values (Table 2).

4.3 Effect of quantitative resistance impacting infection efficiency

As the optimization principle does not hold, the shape of $\mathcal{R}_0$ function alone is not sufficient to characterize evolutionary attractors. PIP must be used instead (Figure S1 for an illustration). In sharp contrast with the SP scenario, two configurations - corresponding to monomorphic or dimorphic populations - are possible.

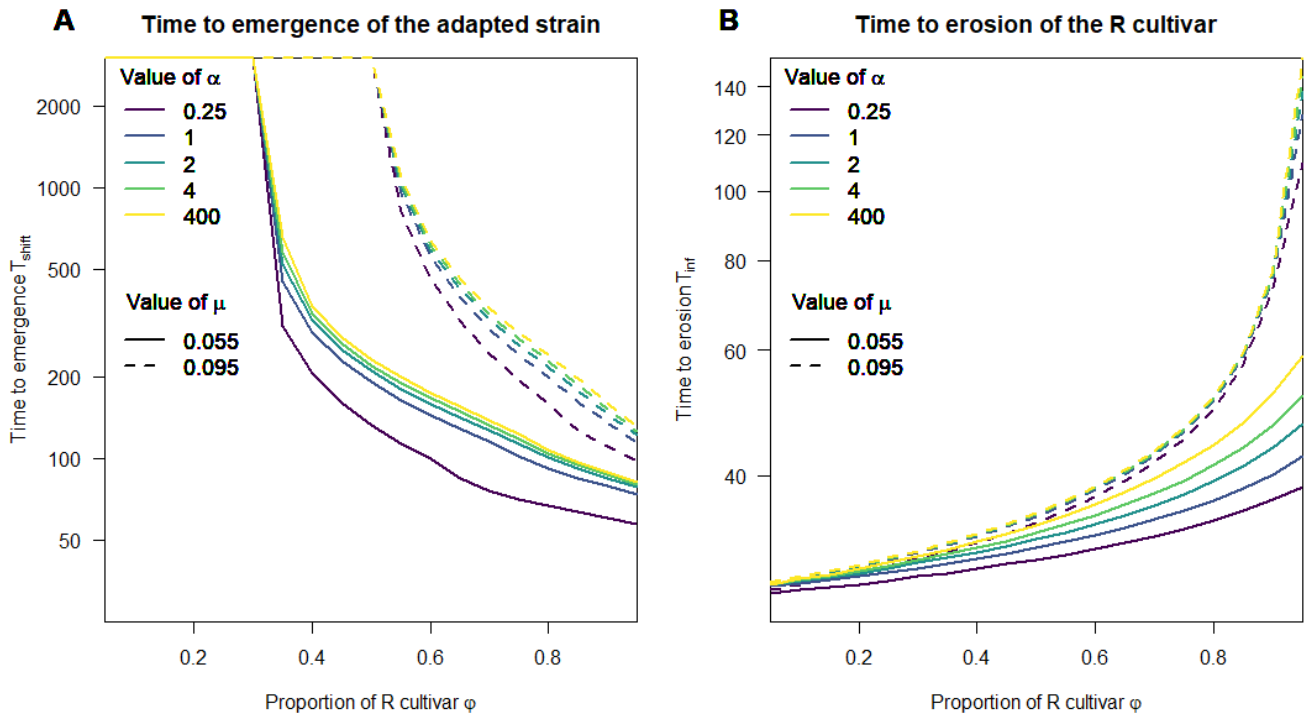

Figure 3: Times to emergence and erosion as a function of the deployment strategies when the resistance impacts the total spore production. **A** Effect of the deployment strategy φ on the time of emergence of the adapted strains T_{shift} for two values of resistance efficiency μ and five shape of the trade-off between sporulation and latency α. Values of T_{shift} are right-censored for $T_{\text{shift}} > 3000$. **B** Same as **A** for the time when the erosion of the quantitative resistance become detectable in the field T_{inf}. For both panels, other parameters are set to their reference values (Table 2).

As previously, the choice of μ and φ can lead to the selection of a single generalist at equilibrium (Figure 4 A-C). But, other choices can lead to the selection of a pathogen population composed of two evolutionary attractors corresponding to specialists of each cultivars (Figure 4 panels D-F). Formally, dimorphism occurs if there exists two constants $a_S, a_R > 0$ defined by system (E.15), and typically quantifying weights of each strain μ_S and μ_R at the equilibrium (Appendix E). In practise, each cultivar is infected by a specific strain. At equilibrium, the pathogen population is composed of different proportions of the two evolutionary attractors μ_S and μ_R (Figure 4 E-F). We insist here that this is not the case for a quantitative resistance targeting sporulation. With such a resistance, the S and R cultivars are then *simultaneously* infected at a given time by the same pathogen strain (Figure 2 D-I).

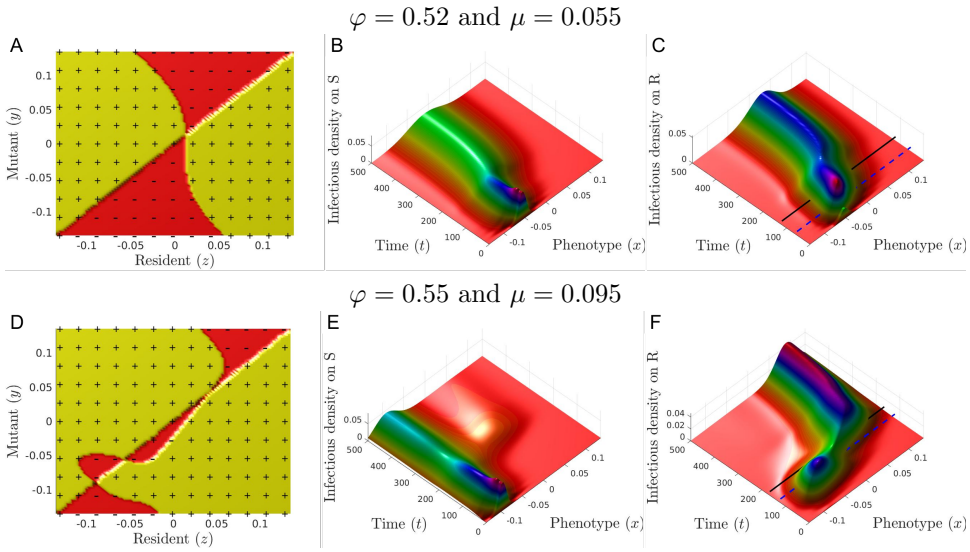

Figure 4: Evolutionary epidemiology dynamics when the resistance impacts the pathogen infection efficiency for two choices of μ and φ. **A-C** With $\mu = 0.055$ and $\varphi = 0.52$, the PIP reveals a single evolutionary attractor μ^* (panel A). The dynamics of the density of infected tissue and the phenotypic composition of the pathogen population in the S and R cultivars are displayed in panels B and C, respectively. The dash-blue and black lines in panel C correspond to T_{inf} and T_{shift}, respectively. **D-F** Same as **A-C** with $\mu = 0.055$ and $\varphi = 0.52$. The PIP reveals two evolutionary attractors μ_S and μ_R. For all panels, $\alpha = 2$, $c = 0$, $\sigma = 5/6$ and other parameters are set to their reference values (Table 2). In panels A and C, singular strategies μ^* and μ_S are evolutionary stable (no nearby mutant can invade): in the PIP, the vertical line through μ^* (panel A), μ_S (panels D) lies completely inside a region marked '$-$', while μ_R is a branching point.

5 Discussion

This work follows an ongoing trend aiming to jointly model the epidemiological and evolutionary dynamics of host-parasite interactions. Our theoretical framework, motivated by fungal infections in plants, allows us to tackle the question of the durability of plant quantitative resistances altering specific pathogen life-history traits. Many problems and questions are reminiscent of the literature on the epidemiological and evolutionary consequences of vaccination strategies. For instance, quantitative resistance traits against pathogen infection rate, latent period and sporulation rate are analogous to partially effective (imperfect) vaccines with anti-infection, anti-growth or anti-transmission modes of action, respectively (Gandon et *al.*, 2001). Similarly, the proportion of fields where a R cultivar is deployed is analogous to the vaccination coverage in the population (Gandon & Day, 2007).

Evolutionary outcomes with multimodal fitness functions. In line with early motivations for developing a theory in evolutionary epidemiology (Day & Proulx, 2004), we investigated both the short- and long-term epidemiological and evolutionary dynamics of the host-pathogen interaction. Although the short-term dynamics is investigated numerically, the long-term analysis is analytically tractable and allows us to predict the evolutionary outcome of pathogen evolution. In contrast with most studies in evolutionary epidemiology, the analysis proposed allows us to consider multimodal fitness functions, and to characterize evolutionary attractors at equilibrium through

a detailed description of their shape (number of modes, steepness and any higher moments with even order). Similarly, our results are neither restricted to Gaussian mutation kernel m (see also Mirrahimi (2017)), provided that m is symmetric and positive (Appendix B), nor to rare mutations as in the classical adaptive dynamics approach. In our work, the SP scenario admits an optimisation principle and potential evolutionary attractors are located at the peaks $\mathcal{R}_0$. This is not always the case for the IE scenario (except for some special configurations). An important consequence of the existence of an optimisation principle is that evolutionary branching (*i.e.* a situation leading to pathogen diversification and to long term coexistence of different pathogen strategies) is impossible.

$\mathcal{R}_0$ expression for fungal pathogens in heterogeneous host environment. Usually, the computation of $\mathcal{R}_0$ is based on the spectral radius of the next generation operator (NGO) (Diekmann et *al.*, 1990). The method was applied by van den Bosch et *al.* (2008) to calculate the $\mathcal{R}_0$ for lesion forming foliar pathogens in a setting with only two cultivars and no effect of the age of infection a on sporulation rate and disease-induced mortality. Here, we follow the methodology based on the generation evolution operator (Inaba, 2012) to derive an expression for the basic reproduction number $\mathcal{R}_0$ in heterogeneous host populations composed of N_c cultivars (Appendix D).

Lannou (2012) pointed out the need for $\mathcal{R}_0(x)$ expressions allowing to compare the fitness of competing pathogen strains with different latent periods. We provide such an expression of $\mathcal{R}_0$ (3.3) for the classical gamma sporulation curve proposed by Segarra et *al.* (2001) and observed for several plant fungi (van den Bosch et *al.*, 1988; Sache et *al.*, 1997; Kolnaar & Bosch, 2011; van den Bosch et *al.*, 1988). This expression combine (i) the pathogenicity traits expressed at plant scale during the basic infection steps (infection efficiency $\beta_k(x)$, latent period $\tau_k(x)$ and shape of the sporulation function $p_k(x)$, $n_k(x)$ and $\lambda_k(x)$) with (ii) the proportion of each cultivar k in the environment (φ_k). As these traits can be measured in the laboratory, $\mathcal{R}_0(x)$ bridges the gap between plant-scale and epidemiological studies, and between experimental and theoretical approaches. $\mathcal{R}_0$-based approach have been for example used to compare the fitness of a collection of isolates of potato light blight (Montarry et *al.*, 2010), to highlight the competition exclusion principle for multi-strains within-host malaria infections (Djidjou-Demasse & Ducrot, 2013) and to predict the community field structure of Lyme disease pathogen from laboratory measures of the three transmission traits (Durand et *al.*, 2017).

$\mathcal{R}_0$ as a proxy of invasion fitness for pathogenicity traits involved in the sporulation curve. In the context of model (2.2) characterized by a common pool of well-mixed airborne pathogen propagules, the function $\Psi(x)$, which is proportional to $\mathcal{R}_0(x)$, is an exact fitness proxy for competing strains differing potentially their sporulation curve (including the latent period, the total spore production and the shape of the sporulation curve). The basic reproduction number $\mathcal{R}_0$ can thus be used to investigate how basic choices made when deploying a new resistance (resistance factor, proportion cultivated) impact the emergence of specialist or generalist pathogen. With a unique local maximum of $\mathcal{R}_0$, a generalist pathogen will be selected while with two local maxima a specialist is selected. But, in any case, the pathogen population will become monomorphic at equilibrium after the deployment of a R cultivar impacting any pathogenicity traits involved in the sporulation curve (*i.e.* expressed after spore germination) as the optimization principle prevents evolutionary branching. This is typically the case in the SP scenario. However, more generally, a clear distinction between pathogen invasion fitness $\mathcal{R}(x, y)$ and epidemiological $\mathcal{R}_0(x)$ is necessary to properly discuss the adaptive evolution of pathogens (Lion & Metz, 2018). Even with a common pool of spore, the optimisation principle of $\mathcal{R}_0(x)$ does not hold when infection efficiencies differ between host classes. It follows that in our case study the deployment of a R cultivar impacting infection efficiency (IE scenario) can lead to the selection of either a monomorphic population with a generalist pathogen or a polymorphic population with two specialist pathogens (Figure 4). The occurrence of such evolutionary branching is of practical importance for management purposes as evidenced for example in the wheat rust fungal disease where disease prevalence varies with the frequencies of specialist genotypes in the rust population (Papaïx et *al.*, 2011).

Our results also highlight that a detailed knowledge of within-host pathogenicity trait correlations is required to manage resistance durability. Only few studies taking explicitly into account evolutionary principles compared how resistant cultivars targeting different aggressiveness components of fungal pathogens impact durability (Iacono et *al.*, 2012; Bourget *al.*, 2015; Rimbaud et *al.*, 2018). These studies assumed that aggressiveness components are mutually independent while correlations have been sometimes identified between latent period and propagule production (Lannou, 2012; Pariaud et *al.*, 2013). We show that such correlations can impact durability when quantitative resistance targets traits involved in the sporulation curve. In the SP scenario, the shape of this correlation finely interacts with the detailed choices of the quantitative resistance factors and their deployment strategies to determine resistance durability (Figure 3 B). Therefore, any guidelines aiming to help plant breeders to adequately choose resistance QTLs in breeding programs should consider these potential correlations. A detailed numerical exploration of the model relying notably on global and local sensitivity analysis could also help to develop

such frameworks both for the questions of breeders ("which resistance factors integrated in breeding scheme ?") and growers ("how to best deploy the existing cultivar portfolio to lower pesticide use ?"). In particular the relative effects of the main components of resistance efficiency (parameters μ, c, σ_S^2 and σ_R^2) and their interactions with φ deserve to be studied in details. Similarly, our results illustrate that the time to emergence of the adapted strain, which corresponds to the duration of the transient dynamic, does not necessarily inform on the time to erosion of a quantitative resistance, in particular when small proportions of R cultivar are deployed (Figure 3). An in-depth analysis of this relationship in a large number of possible states of nature will be interesting.

Notes on some model assumptions. The model assumes an infinitely large pathogen population. Demographic stochasticity is thus ignored while it can impact evolutionary dynamics (*e.g.*, lower probabilities of emergence and fixation of beneficial mutations, reduction of standing genetic variation (Kimura, 1962)). In particular, genetic drift is more likely to impact the maintenance of a neutral polymorphism rather than of a protected polymorphism where selection favors coexistence of different genotypes against invasions by mutant strategies (Geritz et *al.*, 1998). The effect of genetic drift depends on the stability properties of the model considered. As our model has a unique globally stable equilibrium, genetic drift is likely to play a much lesser role than with models characterized by unstable equilibrium. Moreover large N_e in the range $\simeq 10^3$ - 3.10^4 have been reported at field scale for several species of wind-dispersed, spore-producing plant pathogens (Ali et *al.*, 2016; Zhan et *al.*, 2001; Walker et *al.*, 2017), suggesting a weak effect of genetic drift for their evolution.

The model also assumes a unique pool of well mixed propagules. Thus spore dispersal disregard the location of healthy and infected hosts. This assumption, which ensure the one-dimensional environmental feedback loop of the model, is more likely when the extent of the field or landscape considered is not too large with respect to the dispersal function of airborne propagules. Airborne fungal spores often disperse over substantial distances with mean dispersal distance in the range 10^2 to 10^3 meters and, in most case, fat-tail dispersal kernels associated to substantial long-distance dispersal events (Fabre et *al.* (2020) for a review). Recently, a spatially-implicit framework embedded into integro-differential equations was used to describe the eco-evolutionary dynamics of a phenotypically structured population subject to mutation, selection and migration between two habitats (Mirrahimi, 2017). With the same goal Rimbaud et *al.* (2018) used a spatially-explicit framework with n habitats embedded into a SEIR stochastic model. It would be interesting to draw on these examples and extend our approach to a spatially explicit environment. Indeed, when dispersal decreases with distance, large homogeneous habitats promote diversification while smaller habitats, favoring migration between distinct patches, hamper diversification (Débarre & Gandon, 2010; Haller et *al.*, 2013; Papaïx et *al.*, 2013). Managing the resulting population polymorphisms, either for conservation purpose in order to preserve the adpative potential of endangered species or for disease control purpose in order to hamper pest and pathogen adaptation should become a priority (Vale, 2013).

Acknowledgements

Authors thank Ludek Berec, Eva Kisdi and Loup Rimbaud for comments and suggestions to improve the manuscript.

Funding

RDD received support from the Conseil Interprofessionnel du Vin de Bordeaux (CIVB) under the CIVB project 'Recherche, experimentation, etudes et outils', and from the EU in the framework of the Marie-Curie FP7 COFUND People Programme, through the award of an AgreenSkills/AgreenSkills+ fellowship under grant agreement number FP7-609398. QR received support from the cluster SysNum of Bordeaux University.

Code availability

The MATLAB codes used to simulate the model and generate the main figures have been deposited in Dataverse at https://doi.org/10.15454/WAEIMA

Authors' contributions

RDD, AD, JBB and FF planned and designed the research. RDD, AD, JBB and FF conducted analytic tools and numerical experiments. SL and QR critically revised the manuscript and helped draft the manuscript. All authors

gave final approval for publication and agree to be held accountable for the work performed therein.

References

Anderson, P.K., Cunningham, A.A., Patel, N.G., Morales, F.J., Epstein, P.R., and Daszak, P. 2004. Emerging infectious diseases of plants: pathogen pollution, climate change and agrotechnology drivers. Trends Ecol. Evol. 19:535-544.

Ali, S., Soubeyrand, S., Gladieux, P., Giraud, T., Leconte, M., Gautier, A. Mboup, M., Chen, W., Vallavieille-Pope, C,. and Enjalbert, J. 2016. Cloncase: Estimation of sex frequency and effective population size by clonemate resampling in partially clonal organisms. Mol. Ecol. Resour. 16:45-861.

Anderson, R. M. 1991. Populations and infectious diseases: ecology or epidemiology? J. Anim. Ecol. 60:1-50.

Bourget, R., Chaumont, L., Durel, C-E., and Sapoukhina, N. 2008. Sustainable deployment of QTLs conferring quantitative resistance to crops: first lessons from a stochastic model. New Phytol. 206(3):1163–1171

Burie, J. B., Ducrot, A., Griette, Q., and Richard, Q. 2019. Concentration estimates in a multi-host epidemiological model structured by phenotypic traits. arXiv:1910.09385.

Day, T. 2002. Virulence evolution via host exploitation and toxin production in spore-producing pathogens. Ecol. Lett. 5(4):471-476.

Day, T., and Proulx, S. R. 2000. A general theory for the evolutionary dynamics of virulence. Am. Nat. 163(4):e40-63.

Débarre, F., and Gandon, S. 2010. Evolution of specialization in a spatially continuous environment. J. Evol. Biol. 23(5):1090-1099.

Diekmann, O., Heesterbeek, J. A. P., and Metz, J. A. 1990. On the definition and the computation of the basic reproduction ratio $\mathcal{R}_0$ in models for infectious diseases in heterogeneous populations. J. Math. Biol. 28(4):365-382.

Diekmann, O., Jabin, P.E., Mischler, S., and Perthame, B. 2005. The dynamics of adaptation: an illuminating example and a Hamilton-Jacobi approach. Theor. Popul. Biol. 67:257-271.

Dieckmann, U. 2002. Adaptive dynamics of pathogen-host interactions. Pages 39-59 in: Adaptive dynamics of infectious diseases: In pursuit of virulence management. Dieckmann, U., Metz, J.A.J., Sabelis, M.W., and Sigmund, K., eds. Cambridge University Press.

Djidjou Demasse, R., and Ducrot, A. 2013. An age-structured within-host model for multistrain malaria infections. SIAM J. Appl. Math. 73:572-593.

Djidjou-Demasse, R., Ducrot, A., and Fabre, F. 2017. Steady state concentration for a phenotypic structured problem modeling the evolutionary epidemiology of spore producing pathogens. Math. Models Methods Appl. Sci. 27:385-426.

Durand, J., Jacquet, M., Rais, O., Gern, L., and Voordouw, M. J. 2017. Fitness estimates from experimental infections predict the long-term strain structure of a vector-borne pathogen in the field. Sci. Rep. 7(1):1851.

Fabre, F., Coville, J., and Cunniffe, N. J. 2020. Optimising reactive disease management using spatially explicit models at the landscape scale. In: Plant Diseases and Food Security in the 21st Century. Scott, P., Strange, R.N., Korsten, L., and Gullino, M.L., eds. Springer International Publishing.

Gandon, S., Mackinnon, M.J., Nee, S., and Read, A.F. 2001. Imperfect vaccines and the evolution of pathogen virulence. Nature 414(6865):751–756.

Gandon, S. 2004. Evolution of multihost parasites. Evolution, 58(3):455-469.

Gandon, S., and Day, T. 2007. The evolutionary epidemiology of vaccination. J. R. Soc. Interface 4(16):803-817.

Geritz, S.A., Metz, J.A., Kisdi, É., and Meszéna, G. 1997. Dynamics of adaptation and evolutionary branching. Phys. Rev. Lett. 78(10):2024-2027.

Geritz, S.A.H., Kisdi, É., Meszéna, G., and Metz, J.A.J. 1998. Evolutionarily singular strategies and the adaptive growth and branching of the evolutionary tree. Evol. Ecol. 12:35-57.

Gyllenberg, M., and Service, R. 2011. Necessary and sufficient conditions for the existence of an optimisation principle in evolution. J. Math. Biol. 62(3):359-369.

Haller, B.C., Mazzuccco, R., and Dieckmann, U. 2013. Evolutionary branching in complex landscape. Am. Nat. 184(4):e127-141.

Iacono, G.L., van den Bosch, F., and Paveley, N. 2012. The evolution of plant pathogens in response to host resistance: factors affecting the gain from deployment of qualitative and quantitative resistance. J. Theor. Biol. 304:152-163.

Inaba, H. 2012. On a new perspective of the basic reproduction number in heterogeneous environments. J. Math. Biol. 65(2):309-348.

Kennelly, M. M., Gadoury, D. M., Wilcox, W. F., Magarey, P. A., and Seem, R. C. 2007. Primary infection, lesion productivity, and survival of sporangia in the grapevine downy mildew pathogen *Plasmopara viticola*. Phytopathology, 97(4):512-522.

Kimura, M. 1962. On the probability of fixation of mutant genes in a population. Genetics 47:713-719.

Kolnaar, R.W., and Bosch, F.V.D. 2001. Effect of temperature on epidemiological parameters of *Puccinia lagenophorae*. Plant Pathol. 50:363–370.

Lannou, C. 2012. Variation and selection of quantitative traits in plant pathogens. Annu. Rev. Phytopathol. 50:319-338.

Lion, S., and Metz, J. A. J. 2018. Beyond R_0 maximisation: on pathogen evolution and environmental dimensions. Trends Ecol. Evol. 33:75-90.

McDonald, B. A., and Linde, C. 2002. Pathogen population genetics, evolutionary potential, and durable resistance. Annu. Rev. Phytopathol. 40(1):349-379.

Metz, J.A.J., Geritz, S.A.H., Meszéna, G., Jacobs, F.J.A., and van Heerwaarden, J.S. 1996. Adaptive dynamics, a geometrical study of the consequences of nearly faithful reproduction. Pages 183-231 in: Stochastic and spatial Structures of Dynamical Systems. van Strien, S.J., and Verduyn Lunel, S.M., eds. North-Holland, Amsterdam.

Metz, J. A. J., Mylius, S. D., and Diekmann, O. 2008. When does evolution optimise? Evol. Ecol. Res. 10:629–654

Mikaberidze, A., Mundt, C. C., and Bonhoeffer, S. 2016. Invasiveness of plant pathogens depends on the spatial scale of host distribution. Ecol. Appl. 26:1238–1248.

Montarry, J., Hamelin, F.M., Glais, I., Corbière, R., and Andrivon, D. 2010. Fitness costs associated with unnecessary virulence factors and life history traits: evolutionary insights from the potato late blight pathogen *Phytophthora infestans*. BMC Evol. Biol. 10:1-9.

Mirrahimi, S. 2017. A Hamilton–Jacobi approach to characterize the evolutionary equilibria in heterogeneous environments. Math. Models Methods Appl. Sci. 27(13):2425-2460.

Mylius, S. D., and Diekmann, O. 1995. On evolutionarily stable life histories, optimization and the need to be specific about density dependence. Oikos, 74:218-224.

Niks, R. E., Qi, X., and Marcel, T.C. 2015. Quantitative resistance to biotrophic filamentous plant pathogens: concepts, misconceptions, and mechanisms. Annu. Rev. Phytopathol. 53:444-470.

Nowak, M. A., and Sigmund, K. 2004. Evolutionary dynamics of biological games. Science 303(5659):793-799.

Pariaud, B., van den Berg, F., van den Bosch F., Powers, S.J., Kaltz, O., and Lannou, C. 2013. Shared influence of pathogen and host genetics on a trade-off between latent period and spore production capacity in the wheat pathogen, *Puccinia triticina*. Evol. Appl. 6:303–312.

Papaïx, J., Goyeau, H, Du Cheyron, P., Monod, H., and Lannou, C. 2011. Dynamics of adaptation in spatially heterogeneous metapopulations. New Phytol. 191(4):1095-1107.

Papaïx, J., David, O., Lannou, C., and Monod, H. 2013. Dynamics of Adaptation in Spatially Heterogeneous metapopulations. PLoS ONE 8(2):e54697.

Poland, J. A., Balint-Kurti, P. J., Wisser, R. J., Pratt, R. C., and Nelson, R. J. 2009. Shades of gray: the world of quantitative disease resistance. Trends Plant Sci. 14:21-29.

Pilet-Nayel, M.L., Moury, B., Caffier, V., Montarry, J., Kerlan, M.C., Fournet, S., Durel, C.E., and Delourme, R. 2017. Quantitative resistance to plant pathogens in pyramiding strategies for durable crop protection. Front. Plant Sci. 8:21-29.

Raberg, L., Graham, A. L., and Read, A. F. 2009. Decomposing health: tolerance and resistance to parasites in animals. Philos. Trans. R. Soc. Lond., B, Biol. Sci. 364:37–49.

Rimbaud, L., Papaïx, J., Rey, J. F., Barrett, L. G., and Thrall, P.H. 2018. Assessing the durability and efficiency of landscape-based strategies to deploy plant resistance to pathogens. PLoS Comput. Biol. 14(4):e1006067.

Rueffler, C., and Metz, J. A. 2013. Necessary and sufficient conditions for R_0 to be a sum of contributions of fertility loops. J. Math. Biol. 66(4-5):1099-1122.

Sache, I. 1997. Effect of density and age of lesions on sporulation capacity and infection efficiency in wheat leaf rust (*Puccinia recondita* f.sp. tritici). Plant Pathol. 4:581-589.

Segarra, J., Jeger, M. J., and van den Bosch, F. 2001. Epidemic dynamics and patterns of plant diseases. Phytopathology 91(10):1001-1010.

St Clair, D. A. 2010. Quantitative disease resistance and quantitative resistance loci in breeding. Annu. Rev. Phytopathol. 48:247-268.

van den Driessche, P., and Watmough, J. 2008. Further notes on the basic reproduction number. Pages 159-178 in: Mathematical epidemiology. Lecture Notes in Mathematics, vol 1945. Brauer F., van den Driessche P., and Wu J., eds. Springer, Berlin, Heidelberg.

van den Bosch, F., Frinking, H.D., Metz, J.A.J., and Zadoks, J.C. 1988. Focus expansion in plant disease. III: two experimental examples. Phytpathology 78:919–925.

van den Bosch, F., McRoberts, N., van den Berg, F., and Madden, L. V. 2008. The basic reproduction number of plant pathogens: matrix approaches to complex dynamics. Phytopathology 98(2):239-249.

Vale, P. F. 2013. Killing them softly: managing pathogen polymorphism and virulence in spatially variable environments. Trends Parasitol. 29(9):417-422.

Walker, A.S., Ravigne, V., Rieux, A., Ali, S., Carpentier, F., and Fournier, E. 2017. Fungal adaptation to contemporary fungicide applications: the case of *Botrytis cinerea* populations from Champagne vineyards (France). Mol. Ecol. 26:1919-1935.

Zhan, J., Mundt, C.C., and McDonald B.A. 2001. Using restriction fragment length polymorphisms to assess temporal variation and estimate the number of ascospores that initiate epidemics in field populations of *Mycosphaerella graminicola*. Phytopathology 91:1011-1017.

Zhan, J., Thrall, P. H., Papaïx, J., Xie, L., and Burdon, J. J. 2015. Playing on a pathogen's weakness: using evolution to guide sustainable plant disease control strategies. Annu. Rev. Phytopathol. 53:19-43.

A Supplementary figure

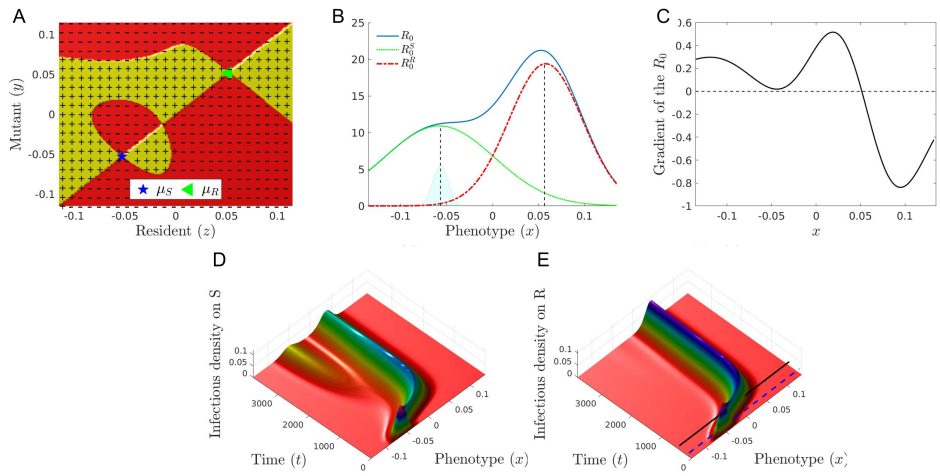

Figure S1: An example of configuration where a polymorphic pathogen population is selected at equilibrium (panels A, D, E) while a single local maximum exists for $\mathcal{R}_0$ (panel B) as confirmed by its gradient (panel C). Parameters values are $\varphi = 0.64$, $\sigma_S = 0.06$, $\sigma = 4/6$, $\mu_S = -\mu_R = -0.0579$, $c = 0$, $\alpha = 2$ and $\varepsilon = 0.01/5$. Other parameters are set to their reference values.

B Properties of the mutation kernel m_ε

The kernel function m_ε arising in model (2.2) should satisfy the following properties:

(H1) The function m_ε is almost everywhere strictly positive on $\mathbb{R}^N$ and should be normalised such that,

$$\int_{\mathbb{R}^N} m_\varepsilon(x)\mathrm{d}x = 1.$$

This last condition expresses that all interactions generated on the phenotypic space of pathogens necessarily end up somewhere on that space.

(H2) Its variation should only depend on the distance separating the points between which the interactions are evaluated (*i.e.* $m_\varepsilon(x) = m_\varepsilon(-x)$, for all $x \in \mathbb{R}^N$).

(H3) It is highly concentrated and decays rather fast at infinity in the sens that $m_\varepsilon(x) = \varepsilon^{-N} m(x/\varepsilon)$ and $m(x) = O\left(\frac{1}{\|x\|^\infty}\right)$ as $\|x\| \to \infty$.

C Some special cases of the general model (2.2)

By omitting the age structure, we re-write model (2.2) as follows

$$\begin{cases} \partial_t S_k(t) = \varphi_k \Lambda - \theta S_k(t) - S_k(t) \displaystyle\int_{\mathbb{R}^N} \beta_k(y) A_k(t,y)\mathrm{d}y, \\ \partial_t i_k(t,x) = \beta_k(x) S_k(t) A(t,x) - \left(\theta + d_k(x) + \dfrac{1}{l_k(x)}\right) i_k(t,x), \\ \partial_t A(t,x) = -\delta A(t,x) + \displaystyle\sum_{k=1}^{N_c} \int_{\mathbb{R}^N} m_\varepsilon(x-y) p_k(y) i_k(t,y)\mathrm{d}y, \end{cases} \tag{C.1}$$

wherein we take into account the (host and strain-specific) duration of the sporulation period, denoted by $l_k(x)$.

Furthermore, if we assume that there are no "interactions" in the phenotypic space of pathogens, *i.e.* without mutations: $\varepsilon \to 0$, then the simplified model (C.1) rewrites

$$\begin{cases} \partial_t S_k(t) = \varphi_k \Lambda - \theta S_k(t) - S_k(t) \displaystyle\int_{\mathbb{R}^N} \beta_k(y) A_k(t,y) \mathrm{d}y, \\ \partial_t i_k(t,x) = \beta_k(x) S_k(t) A(t,x) - \left(\theta + d_k(x) + \dfrac{1}{l_k(x)}\right) i_k(t,x), \\ \partial_t A(t,x) = \displaystyle\sum_{k=1}^{N_c} p_k(x) i_k(t,x) - \delta A(t,x). \end{cases} \tag{C.2}$$

D The fitness function

In this appendix we explain how to compute the fitness function. To that aim, by formally taking the limit $\varepsilon \to 0$ into (2.2), this system becomes

$$\begin{cases} \partial_t S_k(t) = \varphi_k \Lambda - \theta S_k(t) - S_k(t) \displaystyle\int_{\mathbb{R}^N} \beta_k(y) A(t,y) \mathrm{d}y, \\ (\partial_t + \partial_a)\, i_k(t,a,x) = -\left(\theta + d_k(a,x)\right) i_k(t,a,x), \\ i_k(t,0,x) = \beta_k(x) S_k(t) A(t,x), \\ \partial_t A(t,x) = \displaystyle\sum_{k=1}^{N_c} \int_0^\infty r_k(a,x) i_k(t,a,x) \mathrm{d}a - \delta A(t,x). \end{cases} \tag{D.3}$$

Let us assume that system (D.3) reaches a monomorphic epidemiological equilibrium $E^z = (S_k^z, i_k^z(\cdot)\delta_z, A^z\delta_z)_{k=1,\cdots N_c}$, for some trait z, before a new mutation with trait value, say, y occurs. Note that E^z is the environmental feedback of the resident z. We introduce a small perturbation in (D.3) in the phenotype trait y, so that the evolution of the system reads as follows: $S_k(t) = S_k^z + u_k(t)$ and

$$i_k(t,a,x) = i_k^z(a)\delta_z(x) + j_k(t,a)\delta_y(x) \text{ and } A(t,x) = A^z\delta_z(x) + B(t)\delta_y(x),$$

and the small perturbations for the infection, j_k and B, are governed by the linearized system of equations around E^z. This reads as

$$\begin{cases} (\partial_t + \partial_a)\, j_k(t,a) = -\left(\theta + d_k(a,y)\right) j_k(t,a), \\ j_k(t,0) = \beta_k(y) S_k^z B(t), \\ B'(t) = \displaystyle\sum_{k=1}^{N_c} \int_0^\infty r_k(a,y) j_k(t,a) \mathrm{d}a - \delta B(t). \end{cases} \tag{D.4}$$

In order to study the evolution of this perturbation we will derive a renewal equation on $b^z(t,y)$, the density of newly produced spores at time t with phenotype y in the resident population with phenotype x. This term is more precisely defined by

$$b^z(t,y) = \sum_{k=1}^{N_c} \int_0^\infty r_k(a,y) j_k(t,a) \mathrm{d}a.$$

It then follows from the j_k-equation of the linear system (D.4), that

$$j_k(t,a) = \begin{cases} j_k(0,a-t) e^{-\theta t - \int_{a-t}^a d_k(\sigma,y)\mathrm{d}\sigma}, & a \geq t, \\ \beta_k(y) S_k^z B(t-a) e^{-\theta a - \int_0^a d_k(\sigma,y)\mathrm{d}\sigma}, & a < t, \end{cases}$$

while

$$B(t) = \int_0^t b^z(s,y) e^{-\delta(t-s)} \mathrm{d}s + B(0) e^{-\delta t}.$$

As a consequence, $b^z(t,y)$ satisfies the following renewal equation:

$$b^z(t,y) = \sum_{k=1}^{N_c} S_k^z \int_0^t r_k(a,y)\beta_k(y) \int_0^{t-a} b^z(s,y) e^{-\delta(t-a-s)} e^{-\theta a - \int_0^a d_k(\sigma,y)\mathrm{d}\sigma} \mathrm{d}s\mathrm{d}a + \mathcal{F}(t,y,z), \tag{D.5}$$

wherein we have set

$$\mathcal{F}(t,y,z) = \sum_{k=1}^{N_c} \int_t^\infty r_k(a,y) j_k(0,a-t) e^{-\theta t - \int_{a-t}^a d_k(\sigma,y)\mathrm{d}\sigma} \mathrm{d}a$$
$$+ B(0) \sum_{k=1}^{N_c} S_k^z \int_0^t r_k(a,y)\beta_k(y) e^{-\delta(t-a)} e^{-\theta a - \int_0^a d_k(\sigma,y)\mathrm{d}\sigma} \mathrm{d}a.$$

Then (D.5) can be rewritten as

$$b^z(t,y) = \int_0^t B^z(a,y) b^z(t-a,y)\mathrm{d}a + \mathcal{F}(t,y,z),$$

where $B^z(a,y)$ is the expected number of new infections produced per unit time, in a resident host population with phenotype z, by an individual which was infected a units of time ago with the phenotype y, given by

$$B^z(a,y) = e^{-\delta a} \sum_{k=1}^{N_c} S_k^z \beta_k(y) \int_0^a r_k(s,y) e^{\delta s - \theta s - \int_0^s d_k(\sigma,y)\mathrm{d}\sigma} \mathrm{d}s.$$

Due to the above formulation, it follows from classical adaptive dynamics (Diekmann et *al.*, 2005; Geritz et *al.*, 1997; Metz et *al.*, 1996) that the spore numbers, $\mathcal{R}(y,E^z)$, of a rare mutant strategy, y, in the resident z-population is given by

$$\mathcal{R}(y,E^z) = \int_0^\infty B^z(a,y)\mathrm{d}a = \sum_{k=1}^{N_c} S_k^z \Psi_k(y),$$

wherein $\Psi_k(y) = \frac{1}{\delta}\beta_k(y)\int_0^\infty r_k(a,y)\exp\left(-\theta a - \int_0^a d_k(\sigma,y)\mathrm{d}\sigma\right)\mathrm{d}a$. Then, the invasion fitness $f_z(y)$ of a mutant strategy y in the resident z-population is given by

$$f_z(y) = \mathcal{R}(y,E^z) - 1 = \sum_{k=1}^{N_c} S_k^z \Psi_k(y) - 1. \tag{D.6}$$

Note that when the environmental feedback E^z is reduced to the disease-free environment, then S_k^z re-writes as $S_k^z = \frac{\Lambda\varphi_k}{\theta}$. And the epidemiological basic reproduction number of the pathogen with the phenotype y is calculated as

$$\mathcal{R}_0(y) = \frac{\Lambda}{\theta}\Psi(y), \quad \text{with} \quad \Psi = \sum_{k=1}^{N_c} \varphi_k \Psi_k.$$

Once the pathogen has spread and reached the monomorphic equilibrium, then the endemic feedback environment E^z becomes

$$S_k^z = \frac{\Lambda\varphi_k}{\theta + \beta_k(z)A^z}, \quad i_k^z(a) = \beta_k(z)A^z S_k^z \exp\left(-\theta a - \int_0^a d_k(\sigma,z)\mathrm{d}\sigma\right), \tag{D.7}$$

where $A^z > 0$ is the unique solution of the following equation (only defined when $\mathcal{R}_0(z) > 1$):

$$\sum_{k=1}^{N_c} \frac{\Lambda\varphi_k}{\theta + \beta_k(z)A^z}\Psi_k(z) = 1. \tag{D.8}$$

E Dimorphic or monomorphic equilibrium

To simplify the presentation, we consider system (2.2) with $N_c = 2$ corresponding to S and R cultivars. Denote by $(S_0, i_0(\cdot), A_0)$ the endemic equilibrium of system (2.2) as $\varepsilon \to 0$ and when only S is cultivated (*i.e.* when the proportion φ of R is zero). From results in Djidjou-Demasse et *al.* (2017) we have

$$S_0 = \frac{1}{\Psi_S(\mu_S)}. \tag{E.9}$$

Now, let $(S_S, S_R, i_S(\cdot), i_R(\cdot), A)$ be an equilibrium of system (2.2) when a proportion $\varphi > 0$ of R is cultivated. Next recall that, for $k \in \{S, R\}$,

$$S_k = \frac{\varphi_k \Lambda}{\theta + \int_{\mathbb{R}^N} \beta_k(z) A(z) \mathrm{d}z} \text{ and } i_k(x,a) = \beta_k(x) A(x) S_k \exp\left(-\theta a - \int_0^a d_k(\sigma, x) \mathrm{d}\sigma\right),$$

so that $A(\cdot)$ becomes a solution of the nonlinear equation:

$$\int_{\mathbb{R}^N} m_\varepsilon(x-y) \sum_{k \in \{S,R\}} \frac{\varphi_k \Psi_k(y)}{\theta + \int_{\mathbb{R}^N} \beta_k(z) A(z) \mathrm{d}z} A(y) \mathrm{d}y = \frac{1}{\Lambda} A(x). \tag{E.10}$$

Using this equation we heuristically explore conditions yielding to dimorphic or monomorphic equilibrium.

Quantitative resistance impacting infection efficiencies β_S and β_R (IE scenario). We formally assume that the population of spores writes $A(x) = a_S \delta_{\mu_S}(x) + a_R \delta_{\mu_R}(x)$, and we plug this ansatz into equation (E.10) above. This yields, for any x,

$$\begin{aligned}
&a_R \left[\frac{\varphi \Psi_R(\mu_R)}{\theta + a_R \beta_R(\mu_R) + a_S \beta_R(\mu_S)} + \frac{(1-\varphi)\Psi_S(\mu_R)}{\theta + a_R \beta_S(\mu_R) + a_S \beta_S(\mu_S)}\right] m_\varepsilon(x - \mu_R) \\
&+ a_S \left[\frac{\varphi \Psi_R(\mu_S)}{\theta + a_R \beta_R(\mu_R) + a_S \beta_R(\mu_S)} + \frac{(1-\varphi)\Psi_S(\mu_S)}{\theta + a_R \beta_S(\mu_R) + a_S \beta_S(\mu_S)}\right] m_\varepsilon(x - \mu_S) \\
&= \frac{1}{\Lambda} \left[a_R \delta_{\mu_R}(x) + a_S \delta_{\mu_S}(x)\right].
\end{aligned}$$

Letting $\varepsilon \to 0$ and recalling that $m_\varepsilon(x) \approx \delta_0(x)$, one obtains

$$\begin{aligned}
&a_R \left[\frac{\varphi \Psi_R(\mu_R)}{\theta + a_R \beta_R(\mu_R) + a_S \beta_R(\mu_S)} + \frac{(1-\varphi)\Psi_S(\mu_R)}{\theta + a_R \beta_S(\mu_R) + a_S \beta_S(\mu_S)}\right] \delta_{\mu_R}(x) \\
&+ a_S \left[\frac{\varphi \Psi_R(\mu_S)}{\theta + a_R \beta_R(\mu_R) + a_S \beta_R(\mu_S)} + \frac{(1-\varphi)\Psi_S(\mu_S)}{\theta + a_R \beta_S(\mu_R) + a_S \beta_S(\mu_S)}\right] \delta_{\mu_S}(x) \\
&= \frac{1}{\Lambda} \left[a_R \delta_{\mu_R}(x) + a_S \delta_{\mu_S}(x)\right],
\end{aligned}$$

that is

$$\begin{cases}
\dfrac{a_R \varphi \Psi_R(\mu_R)}{\theta + a_R \beta_R(\mu_R) + a_S \beta_R(\mu_S)} + \dfrac{a_R (1-\varphi)\Psi_S(\mu_R)}{\theta + a_R \beta_S(\mu_R) + a_S \beta_S(\mu_S)} = \dfrac{a_R}{\Lambda}, \\
\dfrac{a_S \varphi \Psi_R(\mu_S)}{\theta + a_R \beta_R(\mu_R) + a_S \beta_R(\mu_S)} + \dfrac{a_S (1-\varphi)\Psi_S(\mu_S)}{\theta + a_R \beta_S(\mu_R) + a_S \beta_S(\mu_S)} = \dfrac{a_S}{\Lambda}.
\end{cases}$$

As a consequence, for the equilibrium to be dimorphic, namely $a_R > 0$ and $a_S > 0$, it is necessary that there exist $a_R > 0$ and $a_S > 0$ satisfying the following system of equations:

$$\begin{cases}
\dfrac{\varphi \Psi_R(\mu_R)}{\theta + a_R \beta_R(\mu_R) + a_S \beta_R(\mu_S)} + \dfrac{(1-\varphi)\Psi_S(\mu_R)}{\theta + a_R \beta_S(\mu_R) + a_S \beta_S(\mu_S)} = \dfrac{1}{\Lambda}, \\
\dfrac{\varphi \Psi_R(\mu_S)}{\theta + a_R \beta_R(\mu_R) + a_S \beta_R(\mu_S)} + \dfrac{(1-\varphi)\Psi_S(\mu_S)}{\theta + a_R \beta_S(\mu_R) + a_S \beta_S(\mu_S)} = \dfrac{1}{\Lambda}.
\end{cases}$$

We set

$$\begin{cases}
X = X(a_S, a_R) = \left(\theta + a_R \beta_R(\mu_R) + a_S \beta_R(\mu_S)\right)^{-1}, \\
Y = Y(a_S, a_R) = \left(\theta + a_R \beta_S(\mu_R) + a_S \beta_S(\mu_S)\right)^{-1}.
\end{cases} \tag{E.11}$$

Recall that with the IE scenario we have $r_S = r_R$ and $d_S = d_R$ such that the fitness function $\Psi_k(x) = \frac{1}{\delta} \beta_k(x) \int_0^\infty r_k(a,x) \exp\left(-\theta a\right.$ takes the form $\Psi_k = c_0 \beta_k$ for $k = S, R$ (where c_0 is the same positive funtional for S and R). Doing that, the above system rewrites

$$\mathcal{K}(X,Y)^T = \frac{1}{c_0 \Lambda}(1,1)^T, \tag{E.12}$$

wherein $\mathcal{K} = \begin{pmatrix} \varphi\beta_R(\mu_R) & (1-\varphi)\beta_S(\mu_R) \\ \varphi\beta_R(\mu_S) & (1-\varphi)\beta_S(\mu_S) \end{pmatrix}$ and $c_0 = c_0(\mu_S) = c_0(\mu_R)$. With the IE scenario (*i.e.* with trade-off on infection efficiency β_k), we reasonably have $\beta_R(\mu_R) > \beta_R(\mu_S)$ and $\beta_S(\mu_S) > \beta_S(\mu_R)$. Therefore, $\det(\mathcal{K}) = \varphi(1-\varphi)\left(\beta_R(\mu_R)\beta_S(\mu_S) - \beta_R(\mu_S)\beta_S(\mu_R)\right) > 0$. Then, solving system (E.12) for (X, Y) yields to

$$\begin{cases} X = \dfrac{\beta_S(\mu_S) - \beta_S(\mu_R)}{c_0\Lambda\varphi\left(\beta_R(\mu_R)\beta_S(\mu_S) - \beta_R(\mu_S)\beta_S(\mu_R)\right)} > 0, \\ Y = \dfrac{\beta_R(\mu_R) - \beta_R(\mu_S)}{c_0\Lambda(1-\varphi)\left(\beta_R(\mu_R)\beta_S(\mu_S) - \beta_R(\mu_S)\beta_S(\mu_R)\right)} > 0. \end{cases}$$

Since $\mathcal{R}_0^k(x) = \frac{\varphi_k\Lambda}{\theta}\Psi_k(x) = \frac{\varphi_k\Lambda c_0(x)}{\theta}\beta_k(x)$, the above system rewrites

$$\begin{cases} \theta X = \dfrac{\mathcal{R}_0^S(\mu_S) - \mathcal{R}_0^S(\mu_R)}{\mathcal{R}_0^R(\mu_R)\mathcal{R}_0^S(\mu_S) - \mathcal{R}_0^R(\mu_S)\mathcal{R}_0^S(\mu_R)} > 0, \\ \theta Y = \dfrac{\mathcal{R}_0^R(\mu_R) - \mathcal{R}_0^R(\mu_S)}{\mathcal{R}_0^R(\mu_R)\mathcal{R}_0^S(\mu_S) - \mathcal{R}_0^R(\mu_S)\mathcal{R}_0^S(\mu_R)} > 0. \end{cases}$$

Coming back to the definition of $X = X(a_S, a_R)$ and $Y = Y(a_S, a_R)$ provided by (E.11), we then find

$$\mathcal{G}(a_R, a_S)^T = \left(\frac{1}{X} - \theta, \frac{1}{Y} - \theta\right)^T, \tag{E.13}$$

with $\mathcal{G} = \begin{pmatrix} \beta_R(\mu_R) & \beta_R(\mu_S) \\ \beta_S(\mu_R) & \beta_S(\mu_S) \end{pmatrix}$. Because $\det(\mathcal{G}) = (\beta_R(\mu_R)\beta_S(\mu_S) - \beta_R(\mu_S)\beta_S(\mu_R)) > 0$, it comes that for the equilibrium to be dimorphic it is necessary that

$$\begin{cases} \theta X < 1, \\ \theta Y < 1, \\ \beta_S(\mu_S)\left(\dfrac{1}{\theta X} - 1\right) > \beta_R(\mu_S)\left(\dfrac{1}{\theta Y} - 1\right), \\ \beta_R(\mu_R)\left(\dfrac{1}{\theta Y} - 1\right) > \beta_S(\mu_R)\left(\dfrac{1}{\theta X} - 1\right). \end{cases} \tag{E.14}$$

This heuristic condition (E.14) is necessary (but not sufficient) for system (2.2) (here with $N_c = 2$) to admit an endemic dimorphic equilibrium. The situation with a technical assumption on disjoint supports of β_k, is rigorously studied in Burie *al.* (2019).

But here, in order to go slightly further in our analysis, we assume a strong trade-off on infection efficiency, namely

$$\Psi_l(\mu_k) < 1 \text{ and } \beta_l(\mu_k) \ll 1 \text{ for } l, k = R, S \text{ and } l \neq k.$$

We deduce that the above system of equation roughly simplifies into

$$\begin{cases} \dfrac{\varphi\Psi_R(\mu_R)}{\theta + a_R\beta_R(\mu_R)} \approx \dfrac{1}{\Lambda}, \\ \dfrac{(1-\varphi)\Psi_S(\mu_S)}{\theta + a_S\beta_S(\mu_S)} \approx \dfrac{1}{\Lambda}. \end{cases}$$

Hence the proportions of each phenotype, μ_S and μ_R, can be calculated as

$$a_R \approx \frac{\varphi\Lambda\Psi_R(\mu_R) - \theta}{\beta_R(\mu_R)} \quad \text{and} \quad a_S \approx \frac{(1-\varphi)\Lambda\Psi_S(\mu_S) - \theta}{\beta_S(\mu_S)}, \tag{E.15}$$

provided the following threshold conditions in this strong trade-off framework

$$\varphi\frac{\Lambda}{\theta}\Psi_R(\mu_R) > 1 \text{ and } (1-\varphi)\frac{\Lambda}{\theta}\Psi_S(\mu_S) > 1.$$

Quantitative resistance impacting total sporulation production p_S and p_R (SP scenario). In this case, using the same argument as in Djidjou-Demasse et *al.* (2017) we can prove that the spore population is monomorphic at equilibrium such that $A(x) = a^*\delta_{\mu^*}(x)$; with $a^* > 0$, providing that we are not in a strict symmetric configuration of the fitness function. Moreover, with a strong trade-off on sporulation rate, it is well known that $\mu^* \in \{\mu_S, \mu_R\}$. Then, applying the same arguments as in the previous section lead to

$$\frac{a^*}{\theta + a^*\beta(\mu^*)} m_\varepsilon(x - \mu^*)\Psi(\mu^*) = \frac{a^*}{\Lambda}\delta_{\mu^*}(x).$$

Again with $\varepsilon \to 0$, it comes

$$a^* = \frac{\Lambda\Psi(\mu^*) - \theta}{\beta(\mu^*)} = \frac{\theta}{\beta(\mu^*)}\left[\mathcal{R}_0(\mu^*) - 1\right],$$

with $\mathcal{R}_0(\mu^*) > 1$.

F $\mathcal{R}_0$ as the fitness proxy

By Equations (D.6) and (D.7), it comes

$$f_z(y) = \sum_{k=1}^{N_c} \frac{\Lambda\varphi_k\Psi_k(y)}{\theta + \beta_k(z)A^z} - 1. \tag{F.16}$$

Using Equation (D.8) defining the resident equilibrium, i.e. $\mathcal{R}(z, E^z) = 1$, (F.16) becomes

$$f_z(y) = \sum_{k=1}^{N_c} \frac{\Lambda\varphi_k}{\theta + \beta_k(z)A^z}\left(\Psi_k(y) - \Psi_k(z)\right). \tag{F.17}$$

When infection efficiencies do not differ between host classes (*i.e.* $\beta_k = \beta(x)$, for every k and every x). Then (F.17) gives

$$f_z(y) = \frac{\theta}{\theta + \beta(z)A^z}\left(\mathcal{R}_0(y) - \mathcal{R}_0(z)\right),$$

and then

$$\mathrm{sign}(f_z(y)) = \mathrm{sign}\left(\mathcal{R}_0(y) - \mathcal{R}_0(z)\right). \tag{F.18}$$